

dispersion relation linear in k at long wavelengths (sound waves) but forces a finite “mass” also to the lattice phonons. Allowing for electron screening of the “bare” ion–ion Coulomb interaction, as embodied in the electron gas dielectric function $1/\epsilon(0, q) = q^2/(k_s^2 + q^2)$, one obtains the dressed phonon frequency

$$\omega_q^2 = \frac{\omega_{ip}^2}{\epsilon(0, q)} = \frac{Zm_e}{AM} \frac{\omega_{ep}^2}{q^2 + k_s^2} q^2 = \frac{\omega_{ip}^2}{q^2 + k_s^2} q^2. \quad (3.A.45)$$

The quantity k_s is the Thomas–Fermi screening wave vector, a quantity which is of the order of the Fermi momentum, the associated screening length being then of the order of the Wigner–Seitz radius. Thus,

$$\lim_{q \rightarrow 0} \omega_q = c_s q \quad (3.A.46)$$

where

$$c_s^2 = \frac{Zm_e}{AM} \frac{\omega_{ep}^2}{k_s^2}, \quad (3.A.47)$$

is the sound velocity. Making use of⁸⁵

$$k_s = \left(\frac{6\pi n_e e^2}{\epsilon_F} \right)^{1/2} = \left(\frac{6\pi Zn_i e^2}{\epsilon_F} \right)^{1/2} = \left(\frac{4k_F}{\pi a_0} \right)^{1/2} \approx 1.6 \text{ \AA}^{-1}, \quad (3.A.48)$$

and of (3.A.31), one can write

$$c_s^2 = \frac{Zm_e}{AM} \frac{4\pi n_e e^2}{m_e} \frac{\epsilon_F}{6\pi n_e e^2} = \frac{2Z}{3AM} \epsilon_F = \frac{Zm_e}{3AM} v_F^2, \quad (3.A.49)$$

where use has been made of

$$n_e = \frac{3}{4\pi} \frac{1}{r_s^3} = 4.7 \times 10^{-2} \text{ \AA}^{-3} \quad (r_s = 1.72 \text{ \AA}, \text{Li}) \quad (3.A.50)$$

and

$$\epsilon_F = \frac{50.1}{(r_s/a_0)} \approx 15.42 \text{ eV} \quad (r_s/a_0 = 3.25, \text{Li}), \quad (3.A.51)$$

With the help of

$$k_F = \frac{1.92}{r_s}, \quad (3.A.52)$$

With the help of (3.A.48a)

and of the velocity of light,

$$c = 3 \times 10^{10} \text{ cm/sec}, \quad (3.A.53)$$

⁸⁵cf. Ashcroft and Mermin (1987) Eq. (17.55), Kittel Ch. 8 Eq. (23). It is of notice that the corresponding expression in Ketterson and Song (1999) carries a factor π^2 instead of the correct factor π .

① The quantity (85)

$$\text{top, } k_s = \left(\frac{6\pi n e^2}{\epsilon_F} \right)^{1/2} = \left(\frac{4k_F}{\pi a_0} \right)^{1/2} = 0.82 k_F \left(\frac{r_s}{a_0} \right)^{1/2} \quad (3.A.47)$$

~~272~~ is the Thomas-Fermi screening wave vector, a quantity which of the order of the Fermi momentum, the associated screening length being then of the order of the Wigner-Seitz radius. In writing the above relations use has been made of

$$k_F = \left(\frac{9\pi}{4} \right)^{1/3} \frac{1}{r_s} = \frac{1.92}{r_s}, \quad (3.A.48a)$$

and

$$\epsilon_F = \frac{e^2 a_0}{2} k_F^2, \quad (3.A.48b)$$

In the case of metallic Li ($k_F = 1.12 \text{ \AA}^{-1}$, $r_s = 1.72 \text{ \AA}$),

$$r_s = 1.6 \text{ \AA}^{-1} \quad (3.A.49)$$

Let us return to (3.A.46), and take the the long wavelength limit of ω_q . One finds

$$\lim_{q \rightarrow 0} \omega_q = c_s q$$

the sound velocity (squared) being
to p. ~~272~~



$$\left(\frac{1973.3 \text{ eV} \times \text{\AA}}{0.511 \times 10^6 \text{ eV}} \right) \times 3 \times 10^{10} \frac{\text{cm}}{\text{sec}} \times \frac{1.92}{1.72 \text{ \AA}}$$

3.A. MEDIUM POLARIZATION EFFECTS AND PAIRING

273

one obtains,

$$v_F = \left(\frac{\hbar}{m_e} \right) k_F = \left(\frac{\hbar c}{m_e c^2} \right) \times 3 \times 10^{10} \frac{\text{cm}}{\text{sec}} \frac{1.92}{r_s}$$

$$= \left(\frac{2 \times 10^3 \text{ \AA eV}}{0.5 \times 10^6 \text{ eV}} \right) \times 3 \times 10^{10} \frac{\text{cm}}{\text{sec}} \frac{1.92}{r_s} \approx 1.29 \times 10^8 \frac{\text{cm}}{\text{sec}} \quad (3.A.54)$$

Thus, for Li (⁹Li) Consequently,

$$c_s^2 = \frac{1}{3} \frac{3m_e}{9M} v_F^2 \approx 6 \times 10^{-5} v_F^2, \quad (3.A.55)$$

and

$$c_s \approx 7.8 \times 10^{-3} v_F \approx 1.0 \times 10^5 \frac{\text{cm}}{\text{sec}}. \quad (3.A.56)$$

That is, about a hundredth of the Fermi velocity, or of the order of 10^5 cm/sec, in overall with experimental findings⁸⁶.

Let us now discuss the effective electron-electron interaction. Within the jellium model used above one can write it as

$$V(\mathbf{q}, \omega) = \frac{U_c(q)}{\epsilon(\mathbf{q}, \omega)}, \quad (3.A.57)$$

where the dielectric function

$$\epsilon(\mathbf{q}, \omega) = \frac{\omega^2(q^2 + k_s^2) - \omega_{ip}^2 q^2}{\omega^2 q^2} \quad (3.A.58)$$

contains the effects due to both the ions and the background electrons, while

$$U_c(q) = \frac{4\pi e^2}{q^2} \quad (3.A.59)$$

is the Fourier transform of the bare Coulomb interaction

$$U_c(r) = \frac{e^2}{r}. \quad (3.A.60)$$

For $\omega \gg \omega_{ip}$ one obtains the so called screened Coulomb field,

$$V(\vec{q}, \omega) = \frac{4\pi e^2 n_e}{q^2 + k_s^2} = U_c^{scr}(q), \quad (3.A.61)$$

its \mathbf{r} space Fourier transform being

$$U_c^{scr}(r) = \frac{e^2}{r} e^{-k_s r}. \quad (3.A.62)$$

⁸⁶Ashcroft and Mermin (1987), p. 51, Ketterson and Song (1999) p. 234.

$$\frac{\omega^2 q^2}{\omega^2 (q^2 + k_s^2) - \omega_{ip}^2 q^2} = \frac{\omega^2 q^2}{\omega^2 (q^2 + k_s^2)} \left(\frac{1}{1 - \frac{\omega_{ip}^2 q^2}{\omega^2 (q^2 + k_s^2)}} \right)$$

A quantity that for large values of r falls off exponentially. Thus, in the high frequency limit, the electron-electron interaction, although strongly renormalized by the exchange of plasmons, as testified by the fact that (e.g. for Li),

$$U_c^{scr}(r = 5 \text{ \AA}) \approx U_c(r = 5 \text{ \AA}) e^{-1.6 \times 5} \approx 1 \text{ meV}, \quad (3.A.63)$$

as compared to $U_c(r = 5 \text{ \AA}) \approx 2.9 \text{ eV}$, is still repulsive.

Let us now consider frequencies $\omega \ll \omega_{ip}$ but for values of q of the order of a^{-1} , where a is the lattice constant ($a \approx 3 - 5 \text{ \AA}$, $a^{-1} \approx 0.25 \text{ \AA}^{-1}$) to be compared to $k_s \approx 1.6 \text{ \AA}^{-1}$ and $k_F \approx 1.12 \text{ \AA}^{-1}$ (metallic Li). In the case in which $\omega_{ip}^2/\omega^2 > (q^2 + k_s^2)/q^2$, V is attractive. This behavior explicitly involves the ions through ω_{ip} (electron-phonon coupling).

The dispersion relation of the associated frequency collective modes follows from

$$\text{In other words, } \epsilon(\mathbf{q}, \omega) = 0. \quad (3.A.64)$$

Making use of Eq. (3.A.58) one obtains the relation (3.A.45) as expected. One can now rewrite the reciprocal of the dielectric functions in terms of ω_q , that is,

$$\frac{1}{\epsilon(\mathbf{q}, \omega)} = \frac{\omega^2 q^2}{(q^2 + k_s^2)(\omega^2 - \omega_q^2)} = \frac{q^2}{q^2 + k_s^2} \left[1 + \frac{\omega_q^2}{\omega^2 - \omega_q^2} \right]. \quad (3.A.45)$$

On making

For $\omega \gg \omega_q$ one recovers the Thomas-Fermi dielectric function. For ω near, but smaller than ω_q the interaction is attractive⁸⁷. The effective electron-electron interaction can be then written as

$$V(q, \omega) = \frac{4\pi e^2 n_e}{q^2 + k_s^2} + \frac{4\pi e^2 n_e}{q^2 + k_s^2} \frac{\omega_q^2}{\omega^2 - \omega_q^2} = \frac{4\pi e^2 n_e}{q^2 + k_s^2} + \frac{4\pi e^2 n_e}{q^2 + k_s^2} \frac{\omega_q^2}{\omega^2 - \omega_q^2} \quad \text{es decir}$$

eventually becomes attractive

The quantity where

$$\Pi(q, \omega) = \left(\frac{Z}{AM} \right) \frac{q^2}{\omega^2 - \omega_q^2} \quad (3.A.67)$$

This quantity is intimately connected with Lindhard's function⁸⁸. See also the close relation with the expression (3.A.20) of the nuclear renormalized pairing interaction. The first term of $V(q, \omega)$ contains the screened Coulomb field arising from the exchange of plasmons between electrons (cf. Fig. 3.A.4). The second term with the exchange of collective low frequency phonons calculated making use of the same screened interaction as emerges from (3.A.66).

⁸⁷ Schrieffer (1964), Fig. 6-11, p. 152.

⁸⁸ Lindhard (1953).

In working out the last expression Eqs. (3.A.45) and (3.A.31) have been used. In other words $\omega_q^2 = (Zm_e/AM)(\omega_{ep}^2/(q^2 + k_s^2))q^2 = (Z/AM)(4\pi n_e e^2/(q^2 + k_s^2))q^2$.

224

discussed above 274
to p. 270 270

(Σ) concerning the parallels between pairing in nuclei and in metals, it is also important to point out to the important differences. At least concerning the possibility of developing a unified theoretical working tool.

In metals the bare interaction emerges from the exchange of photons, a process which can be described at profit in terms of an instantaneous Coulomb interaction. While major progress have been made concerning the bare nucleon interaction at large, and the NN-pairing interaction in particular, taking also into account three-body processes and carrying ab initio calculations, we are not yet in possess of the equivalent of the Coulomb interaction. Let alone of a so called low- k version of such interaction, which could allow to work on equal footing Hartree-Fock-Bogoliubov solutions, and QRPA microscopic calculations of low-lying collective modes in the variety of channels (density, spin, charge-exchange, etc.).

Concerning these phonons, they are built of the same nucleon degrees of freedom which already exhaust the nuclear phase space. Double counting and Pauli principle violations have to be taken care of in using the collective modes.

as intermediate bosons. ~~on the~~

In metal, phonons are associated with lattice vibrations, ~~so~~ that is degrees of freedom different from the electronic ones.

(274) v
270 b

On the other hand, the fact that in nuclei one can describe, if not identical, rather similar phenomena as those leading to some of the most remarkable and technically transferable quantum phenomena (persistent currents, high magnetic fields, the Josephson effect),

in terms of individual
quantal states and of
~~single~~ cooper pairs,

makes of the nuclear ~~paradigm~~ ^{pairing} a unique laboratory of many-body physics, ~~from~~
~~which practice~~

(Σ)

fermion materials

p.274

~~myle molecule etc~~

~~old version etc~~

~~pygmy~~

~~p. 270~~

~~274~~

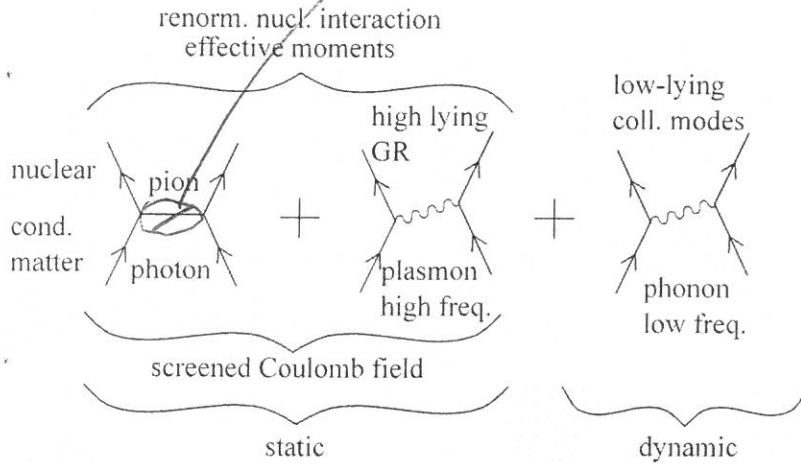


Figure 3.A.4: Schematic representation of the variety of contributions to the effective interaction in nuclei and in metals.

Let us now introduce the dimensionless quantity

$$\lambda = \langle F|V|I \rangle = N(0)U_c^{scr}(1 + U_c^{scr}\Pi). \quad (3.A.68)$$

In the weak coupling limit ($\lambda^2 \ll \lambda$)

$$\Delta = 2\omega_D e^{-1/\lambda}, \quad (3.A.69)$$

where ω_D is the Debye energy. Now, provided that we are in a situation in which ω is consistently different from ω_q ,

$$\frac{1}{\lambda} = \frac{1}{N(0)U_c^{scr}(1 + U_c^{scr}\Pi)} \approx \frac{1}{N(0)U_c^{scr}}(1 - U_c^{scr}\Pi), \quad (3.A.70)$$

Thus

$$\frac{1}{\lambda} = \frac{1}{N(0)U_c^{scr}} - \frac{\Pi}{N(0)}, \quad (3.A.71)$$

and

$$\Delta = \left(2\omega_D e^{\frac{\Pi}{N(0)}}\right) e^{-\frac{1}{N(0)U_c^{scr}}}. \quad (3.A.72)$$

Consequently, the renormalization effects of the pairing gap associated with phonon exchange are independent of the approximation used to calculate U_c^{scr} (Thomas-Fermi in the above discussion), provided one has used the same “bare” (screened) Coulomb interaction to calculate ω_q^2 . Otherwise, the error introduced through a resonant renormalization process entering the expression of e.g. the pairing gap may be quite large.

E_{corr}

System	Δ_0		N_0		W_{con}		E_c	BE/A	$\frac{W_{con}}{E_c}$	$\frac{W_{con}}{BE}$
	meV	MeV	$\frac{\text{mev}^{-1}}{\text{atom}}$	MeV^{-1}	$\frac{\text{mev}}{\text{atom}}$	MeV			$\frac{\text{mev}}{\text{atom}}$	$\frac{\text{MeV}}{A}$
Pb ¹²⁰ Sn	1.4	1.5	276	4	3×10^{-4}	4.3	2030	8.5		

Table 3.A.1: Summary of the quantities entering the calculation of the condensation energy superconducting lead (Pb), and of the single open shell superfluid nucleus ¹²⁰Sn.

3.A.4 Pairing condensation (correlation) energy beyond level density

The condensation energy, namely the energy difference $W_N - W_S$ between the normal N - and superfluid S -state is defined as (Eq. (2-35) of ref⁸⁹)

$$W_{con} = W_N - W_S = \frac{1}{2} N(0) \Delta_0^2, \quad (3.A.73)$$

where $N(0)$ is the density of single-electron states of one-spin orientation evaluated at the Fermi surface (p. 31 of ref.⁹⁰), and Δ_0 is the pairing gap at $T = 0$.

The correlation energy E_{corr} introduced in equation (6-618) of ⁹¹

$$E_{corr} = -\frac{1}{2d} \Delta^2 \quad (3.A.74)$$

to represent $W_S - W_N$ in the nuclear case, was calculated making use of a (single particle) spectrum of two-fold degenerate (Kramer degeneracy) equally spaced (spacing d) single-particle levels. Consequently, $2/d$ corresponds to the total level density, and $1/d = N(0)$. In keeping with the fact that a nucleus in the ground state (or in any single quantal state), is at zero temperature, (3.A.73) coincides with (3.A.74), taking into account the difference in sign in the definitions.

Nuclei

The empirical value of the level density parameter for both states (v, \bar{v}) (Kramers degeneracy, both spin orientations) is $a = A/8 \text{ MeV}^{-1}$, $A = N + Z$ being the mass number. Thus, for neutrons one can write $a_N = N/8$ and $N_N(0) = N/16 \text{ MeV}^{-1}$. For ¹²⁰Sn, $N_N(0) \approx 4 \text{ MeV}^{-1}$. Because $\Delta = 1.46 \text{ MeV}$, (Table 3.A.1)

$$W_{con} = \frac{1}{2} \times 4 \text{ MeV}^{-1} \times (1.46)^2 \text{ MeV}^2 \approx 4.3 \text{ MeV}. \quad (3.A.75)$$

The binding energy per nucleon is $BE/A = 8.504 \text{ MeV}$. Thus $BE = 120 \times 8.504 \text{ MeV} = 1.02 \times 10^3 \text{ MeV}$, and

$$\frac{W_{con}}{BE} \approx 4.2 \times 10^{-3}. \quad (3.A.76)$$

⁸⁹ Schrieffer (1964).

⁹⁰ Schrieffer (1964).

⁹¹ Bohr, A. and Mottelson (1975).

Superconducting lead

Making use of the value⁹²

$$N(0) = \frac{0.276 \text{ eV}^{-1}}{\text{atom}}, \quad (3.A.77)$$

and of $\Delta_0 = 1.4 \text{ meV}$, one obtains

$$W_{\text{coh}} = 0.27 \times 10^{-6} \text{ eV/atom}. \quad (3.A.78)$$

In keeping with the fact that the cohesive energy of lead, namely the energy required to break all the bonds associated with one of its atoms is

$$E_{\text{cohe}} = E_c = 2.03 \frac{\text{eV}}{\text{atom}}, \quad (3.A.79)$$

one obtains

$$\frac{W_{\text{coh}}}{E_c} \approx 1.3 \times 10^{-7}. \quad (3.A.80)$$

The different quantities are summarized in Table 3.A.1.

3.A.5 Hindsight

The function $\Pi(q, \omega)$ essentially at resonance ($\omega \lesssim \omega_q$) and its nuclear analogue being $\Pi(\omega, \omega_\alpha)$ again close to resonance ($\omega \lesssim \omega_\alpha$), are the sources of new physics eventually leading to observable emergent properties, provided one finds the proper embodiments. In the case of metals at low temperature there are permanent magnetic fields in a superconducting ring, the Josephson effect, etc. In the case of halo neutron drip line nuclei one finds (see Sect. 3.C in particular paragraph before Eq. (3.C.6)) symbiotic pair addition modes, essentially equality of the absolute one- and two-particle transfer cross sections, etc.

In Fig. 3.A.5 we present a schematic parallel between the physical mechanisms at the basis of the origin of pairing in metals and in nuclei, and of some of the consequences associated with spontaneous breaking of gauge symmetry in these systems, in particular Cooper pair tunneling.

H₄, phenomenon at the basis of the Josephson effect.

Appendix 3.B Cooper pair: radial dependence

The fact that one is still trying to understand (BCS-like) pairing (abnormal phenomena) in nuclei is, to a non negligible extent, due to the fact that, as a rule, pairing in these systems is constrained to manifest itself subject to a very strong "external" (mean, normal density) field⁹³. Also, to some extent, due to the fact that

⁹²Beck and Claus (1970).

⁹³c.f. e.g. Matsuo, M. (2013).

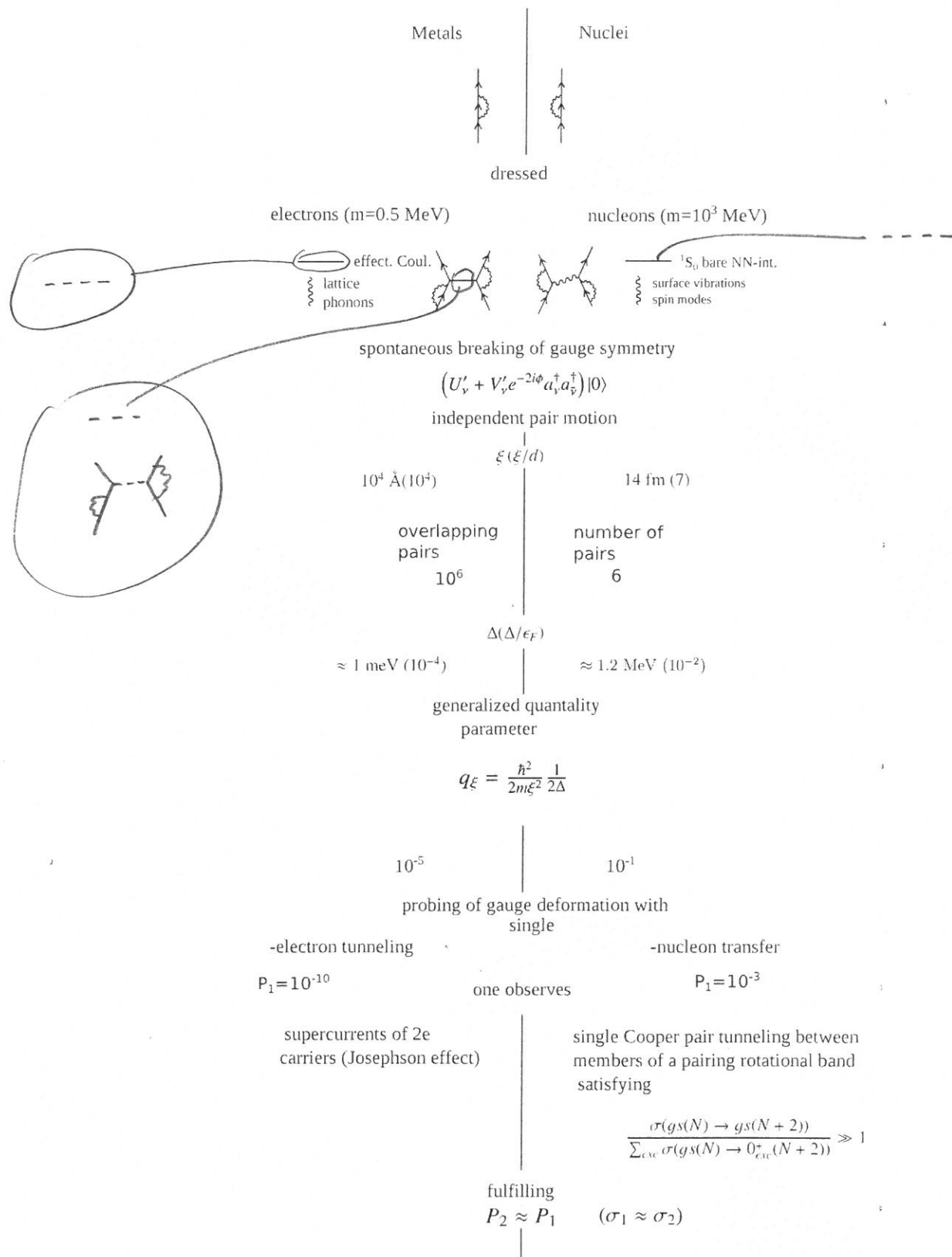


Figure 3.A.5

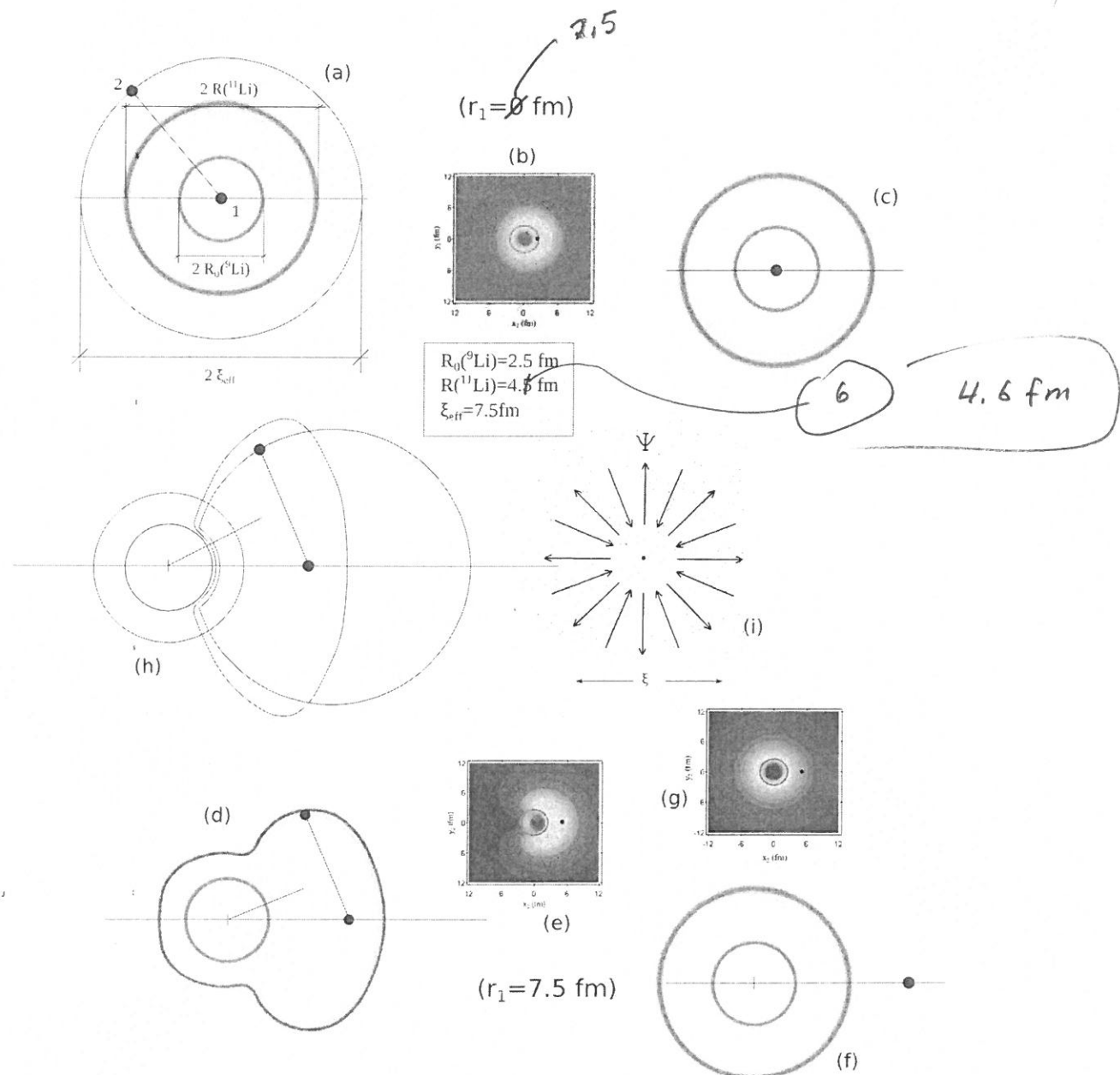


Figure 3.B.1

(as a rule)

the analysis of two-nucleon transfer data was made in terms of relative cross sections and not absolute cross sections as done now⁹⁴. Within this context, Cooper pair transfer was viewed as simultaneous transfer, successive implying a breakup or, at least an anti-pairing disturbance of the pair. There exist a number of evidences which testify to the fact that the picture in which nucleon Cooper pairs are viewed as independent correlated entities over distances of the order of tens of fm (Fig. 3.2.1), contains a number of correct elements (see e.g. Fig. 3.B.1). In this Appendix an attempt at summarizing these evidences, already mentioned or partially discussed above, is made⁹⁵.

The problem that Cooper solved was that of a pair of electrons which interact above a quiescent Fermi sea with an interaction of the kind that might be expected due to phonon exchange and a screened Coulomb field⁹⁶. What he showed approximating this retarded interaction by a non-local one, active on a thin energy shell near (above) the Fermi surface⁹⁷, was that the resulting spectrum has an eigenvalue $E = 2\epsilon_F - 2\Delta$, regardless how weak the interaction is, and consequently the binding energy 2Δ of the pair, so long as the interaction is attractive. This result is a consequence of the Fermi statistic and of the existence of a Fermi sea background – the two electrons interact with each other but not with those in the sea, except via the Pauli principle – since it is known that binding does not ordinarily occur in the two-body problem in three dimensions, until the strength of the attraction exceeds a finite threshold value.

The wavefunction of the two electrons can be written as

$$\Psi(\mathbf{r}_1\sigma_1; \mathbf{r}_2\sigma_2) = \phi_q(\mathbf{r})e^{i\mathbf{q}\cdot\mathbf{R}}\chi(\sigma_1, \sigma_2) \quad (3.B.1)$$

where $\mathbf{R} = (\mathbf{r}_1 + \mathbf{r}_2)/2$, $\mathbf{r} = \mathbf{r}_1 - \mathbf{r}_2$, and σ_1 and σ_2 denote the spins⁹⁸.

Let us consider the state with zero center of mass ($q = 0$) and with zero relative momentum, so that the two electrons carry equal and opposite momenta, aside of being in the singlet spin state state, with

$$\chi = \frac{1}{\sqrt{2}} \left[\begin{pmatrix} 1 \\ 0 \end{pmatrix} \begin{pmatrix} 0 \\ 1 \end{pmatrix} - \begin{pmatrix} 0 \\ 1 \end{pmatrix} \begin{pmatrix} 1 \\ 0 \end{pmatrix} \right] \quad (3.B.2)$$

⁹⁴ See Potel, G. et al. (2013a) and references therein.

⁹⁵ Of course such manifestation will be latent, expressing themselves indirectly. In other words, abnormal density can only be present when normal density, at ever so low values already is present. The pairing field does not have within this context an existence by itself uncoupled from the normal density. On the other hand this, in most cases latent (virtual), and in only few cases factual existence, has important consequences on nuclear properties. Within this context one can mention that the neutron halo normal density in ^{11}Li is not there before the associated abnormal density is operative. In fact abnormal density requires the normal one to develop in this neutron dripline nucleus, and viceversa.

⁹⁶ Cooper (1956).

⁹⁷ States below the Fermi surface are frozen because of Pauli principle.

⁹⁸ In the limit $q \rightarrow 0$ the relative coordinate problem is spherically symmetric so that $\phi_0(\mathbf{r})$ is an eigenfunction of the angular momentum operator (Schrieffer (1964)).

in this case

We have thus a pair of electrons moving in time reversal states and can write⁹⁹,

$$\phi_0(\mathbf{r}) = \sum_{k>k_F} g(\mathbf{k}) e^{i\mathbf{k}\cdot\mathbf{r}} = \sum_{k>k_F} g(\mathbf{k}) e^{i\mathbf{k}\cdot\mathbf{r}_1} e^{-i\mathbf{k}\cdot\mathbf{r}_2}. \quad (3.B.3)$$

In the above wavefunction Pauli principle ($k > k_F$) and translational invariance (dependence on the relative coordinate \mathbf{r}) are apparent. The pair wavefunction is likely a superposition of one-electron levels with energies of the order of 2Δ close to ϵ_F , since tunneling experiments indicate that for higher energies the one-electron density is little altered from the form it has in normal metals. The spread in momenta of the single-electron levels entering (3.B.3) is thus fixed by the condition

$$2\Delta \approx \delta E \approx \delta \left(\frac{p^2}{2m} \right)_{\epsilon_F} \approx v_F \delta p. \quad (3.B.4)$$

Consequently

$$\frac{\delta p}{p_F} = \frac{2\Delta}{mv_F^2} = \frac{\Delta}{\epsilon_F} \ll 1. \quad (3.B.5)$$

Thus, $\phi_0(\mathbf{r})$ consists mainly of waves of wavenumber k_F . Now, because the wavefunction of a Cooper pair represents a bound s -state, the motion it describes is a periodic back and forth movement of the two electrons in directions which are uniformly distributed, covering a relative distance ($\delta x \delta p = \hbar$)

$$\xi = \delta x = \frac{\hbar}{\delta p} = \frac{\hbar v_F}{2\Delta} \quad (3.B.6)$$

as schematically¹⁰⁰ shown in Fig. 3.B.1 (i). It is analogous to the motion of the two nucleon in a deuteron or the main ($L = 0$) component of the two neutrons in the triton. The hydrogen atom in s -state is also an example; in that case it is the electron that does most of the back and forth moving, whereas the proton only recoils slightly.

In keeping with the above arguments and with (3.B.6), $\phi_0(\mathbf{r})$ will look like $e^{i\mathbf{k}_F \cdot \mathbf{r}}$ for $r \ll \xi$, while for $r \gg \xi$ the waves $e^{i\mathbf{k} \cdot \mathbf{r}}$ weighted by $g(k)$ will destroy themselves by interference (Fig. 3.B.2). From the above physical arguments, $\phi_0(\mathbf{r})$ will look like $e^{i\mathbf{k}_F \cdot \mathbf{r}}$ for $r \ll \xi$ while for $r \gtrsim \xi$ one can approximate the weighing function as,

$$g(k) \sim \delta(\mathbf{k}, \mathbf{k}_F + i\hat{\mathbf{k}}_F/\xi), \quad (3.B.7)$$

where $\hat{\mathbf{k}}_F$ is a unit vector. One then obtains,

$$\phi_0(\mathbf{r}) \sim e^{-r/\xi} e^{i\mathbf{k}_F \cdot \mathbf{r}}. \quad (3.B.8)$$

⁹⁹In other words, one expands the $l = 0$ wavefunction ϕ_0 in terms of s -states of relative momentum k and total momentum zero.

¹⁰⁰Weisskopf (1981).

Because we are dealing with a singlet state, and the total wavefunction has to be antisymmetric,

$$\phi_0(\mathbf{r}) \sim e^{-r/\xi} \cos k_F r, \quad (3.B.9)$$

A more proper solution of the Cooper pair problem leads to¹⁰¹

$$\phi_0(\mathbf{r}) \sim K_0(r/\pi\xi) \cos k_F r, \quad (3.B.10)$$

where K_0 is the zeroth-order modified Bessel function. For $x \gg 0$, $K_0(x) \sim (\pi/2x)^{1/2} \exp(-x)$, where $x = r/\pi\xi$.

A wavefunction which extends over distances much larger than the binding potential is a well-known phenomenon when the binding energy is small. For example, as in the case of the deuteron mentioned above.

Be as it may, the large size of the Cooper pair wavefunction also explains why the electrostatic repulsion between electron pairs does not appreciably influence the binding. The repulsion acts only over distances of the order of the correlation length.

Going back to Fig. 3.B.1, it is illustrative to compare the two (NFT calculated) situations displayed in (b) and (e), concerning the relative distribution of the halo neutrons of ^{11}Li . Pairing correlations being, in particular in this case, mainly a surface phenomenon bring, for $r_1 = 7.5$ fm, the two nucleons close to each other as compared to the uncorrelated situation (diagram (g)). The fact that this result, which is not under discussion, is more subtle than just expressed, emerges by looking at (h), where the situation displayed in (b) and (e) (see also (a) and (d)), are schematically drawn in a single plot.

The pairing, Cooper pair phenomenon (dashed curve) implies that the two neutrons recede from each other. However, the average potential $U(r) = \int d\mathbf{r}' v(|\mathbf{r} - \mathbf{r}'|)$ acting as a strong external field which determines where normal ($\rho(r)$), and thus abnormal density can find themselves, distorts the halo Cooper pair, leading to the situation represented with the continuous (irregular) curve. Thus, to a situation in which the two halo neutrons have come closer to each other as compared to the uncorrelated situation. And to do so, the finite quantal system under discussion uses the mechanism discussed in App. 3.D (spatial quantization, i.e. independent particle motion, opposed to independent pair motion).

Now, the situation depicted in Fig. 3.B.1 (e) is not observable with the specific probe, namely a two-particle pick up reaction ($^1\text{H}(^{11}\text{Li}, ^9\text{Li})^3\text{H}$). In fact, during the period of time the proton is around the grazing distance, and one of the halo neutrons joins it to form a virtual deuteron, the situation will essentially evolve into the density distribution represented with the dashed curve in (h), the two members of the halo Cooper pair being at a distance of the order of the correlation length and carrying a much lower relative momentum than that typical of the situation (e) (continuous irregular curve). It is natural that successive transfer dominates the absolute differential cross section.

¹⁰¹Kadin (2007).

*the other neutron ~~electrons~~ can be
at the antipode, essentially one
diameter apart.*

Caption Fig 3.B.1

Synthesis of the spatial structure of ^{11}Li neutron halo Cooper pair calculated in NFT (Barranco, F. et al. (2001)). To make more direct the comparison between the simple estimates and the results of the above reference, it is assumed that $\xi = 7.5$ fm (dashed circle) instead¹⁰² of ≈ 12 fm. Diagrams (a) and (d) are the schematic representations of the modulus square $|\Psi_0(\mathbf{r}_1, \mathbf{r}_2)|^2 = |\langle \mathbf{r}_1, \mathbf{r}_2 | 0 \rangle|^2$ describing the motion of the two halo neutrons of ^{11}Li , moving around the ^9Li core as a function of the cartesian coordinates of neutron 2, for fixed (small and large as compared to $R(^{11}\text{Li})=4.6$ fm) values of the position r_1 of neutron 1 (for more details see Caption to Fig. 2.6.3). Diagrams (b), (e) and (g) are the results of NFT (see also Fig. 2.6.3 (II) a and b)). (a) The circles drawn with continuous lines correspond to the relative distance r at the radius of the ^9Li core and of ^{11}Li . The Cooper pair “intrinsic coordinate” r_{12} is also shown. Particle 1 of the Cooper pair is assumed to occupy the center of the nucleus ($r_1 = 0$). (b) Result of NFT for a situation similar to the above. (c) Schematic representation of an uncorrelated pair in a potential weakly binding the pure configuration $p_{1/2}^2(0)(r_1 = 0)$. (d) Same as (a) but for $r_1 = 7.5$ fm. (e) Result of the NFT calculation for this setup. (f) Schematic representation of a pure configuration $p_{1/2}^2(0)(r_1 = 7.5$ fm). (g) The result of the microscopic calculation for a weakly bound $p_{1/2}^2(0)$ configuration ($r_1 = 7.5$ fm). (h) The variety of situations found in (a) and (d) in comparison to each other in a single cartoon. (i) Schematic picture of the dynamics of the partners fermions in the quantum state of the Cooper pair. It is a linear combination of motions away and towards one another. The fermions stay within a distance of the order ξ , root mean square radius of the Cooper pair (After Weisskopf (1981), see also Kadin (2007) and van Witsen (2014)).

Within the nuclear scenario, to interact at profit through long wavelength medium polarization pairing, pairs of nucleons have to have low momentum. To do so they have to reduce the effect of the strong external (mean) field by moving away from it, possible mechanisms being among others: halo (Fig. 3.B.1), transfer processes (see e.g. Fig. 3.4.1), exotic decay¹⁰³ (see Fig. 3.B.3) and, if nothing else, some amount of spill out.

¹⁰²In connection with this figure we have estimated the Fermi momentum associated with the two halo neutrons of ^{11}Li as $k_F = [(3\pi^2 / ((4\pi/3)((4.6)^3 - (2.5)^3)))^{1/3}] \approx 0.56$, the denominator being the volume associated with the halo. Thus $(v_F/c) \approx 0.2(k_F)_{\text{fm}^{-1}} \approx 0.1$ and $\xi = \hbar v_F / (\pi \times 0.5 \text{ MeV}) \approx 12$ fm (see also Eq. (3.C.5) as well as the end of caption to Fig. 3.B.3; see also App. 6.E).

¹⁰³In Fig. 3.B.3, a parallel is made between correlation lengths associated with (pairing) particle-particle or hole-hole modes and particle-hole vibrations. These last modes also display a consistent spatial correlation (see e.g. Broglia et al. (1971)).

correct $k_F = (3\pi^2 \times 2 / ((4\pi/3)(4.6)^3 - (2.5)^3))^{1/3} \approx 0.56$

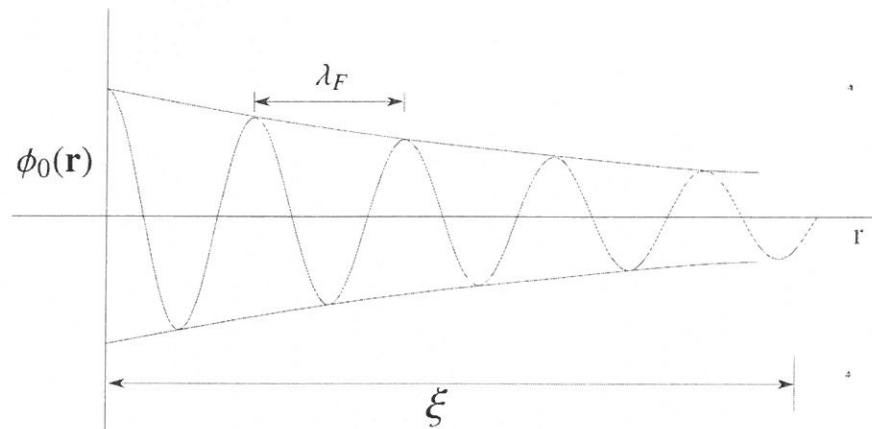


Figure 3.B.2: Schematic representation of the Cooper pair wavefunction. Indicated are the coherence length ξ and the Fermi wavelength $\lambda_F = h/p_F = 2\pi/k_F$. In the nuclear case, and for nuclei along the stability valley $\lambda_F \approx 4.6$ fm and $\xi \approx \hbar v_F/\pi\Delta \approx 14$ fm ($k_F \approx 1.36$ fm⁻¹, $v_F/c \approx 0.27$, $\Delta \approx 1.2$ MeV). Thus $\xi/\lambda_F \approx 3$ (after Weisskopf (1981)).

3.B.1 Number of overlapping pairs

$$0.3 \times 10^{-4}$$

if

The coherence length for low temperature superconductors is of the order of 10^4 Å. In fact, in the case of e.g. bulk Pb, for which ¹⁰⁴ $\Delta = 1.4$ meV and $v_F = 1.83 \times 10^8$ cm/s one obtains $\xi \approx 0.310^{-4}$ cm.

Since electrons in metals typically occupy a volume of the order of $(2\text{\AA})^3$ (Wigner-Seitz cell), there would be of the order of $^{105} \xi^3/(2\text{\AA})^3 \approx 10^4$ other electrons within a "coherence volume". Eliminating the electrons deep within the Fermi sea as they behave essentially as the metal was in the normal phase¹⁰⁶, one gets¹⁰⁷ $\approx 10^6$. In other words, about a million of other Cooper pairs have their center of mass falling inside the coherence volume of a pair. Thus, the isolated pair picture (Fig. 2.3.4) is not correct, but yes that displayed in Fig. 2.3.5.

¹⁰⁴ The experimental value of the critical temperature for Pb is $T_c = 7.193$ K ($k_B T_c = 0.62$ meV). Then $\Delta_0(0)/k_B T_c = 2.26$, to be compared with the BCS prediction of 1.76.

¹⁰⁵ Ketterson and Song (1999) p. 198.

¹⁰⁶ The BCS ground state at $T = 0$ consists in two classes of electrons: those deep inside the Fermi sea, which behave essentially in the same way as those in the normal state, and those near the Fermi surface, which form the overlapping Cooper pairs. These latter electrons cannot scatter because they are in a coherent state. The former electrons inside the sea cannot scatter either because being far from the Fermi surface, they are blocked by Pauli principle. At $T = 0$, all electrons of both classes contribute to the lossless supercurrent Waldrum (1996).

¹⁰⁷ Schrieffer (1964) p. 43. The relative number of the electrons participating in Cooper pair formation can be estimated to be $(\Delta/\epsilon_F \approx 2.8 \text{ meV}/9.47 \text{ eV} \approx 3 \times 10^{-4})$.

$$\text{That is } 3 \times 10^9 \times (2\Delta/\epsilon_F) \approx 10^6$$

$$\text{That is } 3 \times 10^9 \times (2\Delta/\epsilon_F) \approx 10^6 (2\Delta/\epsilon_F \approx \dots)$$

$$\begin{aligned} \Delta/\epsilon_F & \text{ meV} \\ & \approx 1/10 \text{ eV} \\ & = 10^{-4} \end{aligned}$$

($= aS/V$, a being the nuclear diffusivity) is much larger¹⁰⁹ (≈ 0.72) than in the case of heavy nuclei lying along the stability valley (≈ 0.28 in the case of ^{210}Pb). 27

3.B.2 Coherence length and quantality parameter for (ph) vibrations

As seen from Fig. 1.2.2, both $\beta = 0$ and $\beta = \pm 2$ modes lead to a sigmoidal shape of the single-particle occupation probabilities within an energy region $\delta\epsilon = |E_{corr}|$ around the Fermi energy. Consequently, the arguments used in Sect. 3.4.1 and leading to

$$\xi = \frac{\hbar v_F}{\pi |E_{corr}|}, \quad (3.B.12)$$

for pairing modes and resulting in

$$\xi = \frac{\hbar v_F}{\pi \Delta} \quad (3.B.13)$$

for the case of superfluid nuclei, can be used equally well in connection with $\beta = 0$ modes. In other words, in a similar way in which pair addition and subtraction modes (Cooper pairs) can be viewed as correlated pp and hh modes over distances of the order ξ , $\beta = 0$ collective vibrations can be pictured as ph modes correlated again over distances inversely proportional to the correlation energy of e.g. the RPA collective roots. Summing up, ξ describe, both in the case of $\beta = \pm 2$ and $\beta = 0$ modes, a similar physical property of the vibration: the length over which pairs of fermions are correlated in normal $((ph), (pp), (hh))$ or in superfluid $(\cancel{(pp)} \parallel \cancel{(hh)})$ nuclei (see Fig. 3.B.3). *Within this context, let us provide* and

Caption Fig 3.B.3

Vibrations can be classified by the transfer quantum number β . Collective modes with $\beta = 0$ correspond to correlated particle-hole (ph) excitations. For example low-lying quadrupole or octupole (surface) vibrations. Modes with $\beta = \pm 2$ correspond to correlated (pp) or (hh) modes, that is, pair addition and pair subtraction modes. Thinking of these modes propagating in uniform nuclear matter, the associated correlation length can be calculated making use of Eq. (3.B.12), the correlation energy being, as a rule estimated from the shift of the lowest root of the RPA solution for both, ph and pairing modes, from the lowest unperturbed configuration (pole). The (generalized) quantality parameter, ratio of the quantal kinetic energy of localization and the correlation energy, gives a measure of the tendency to independent particle ($q_\xi \approx 1$) or independent pp , hh , ph ($q_\xi \ll 1$) motion. This is in keeping with the fact that potential energy is best profited by special arrangements between nucleons and thus lower symmetry than the original Hamiltonian, while fluctuations favor symmetry. A concrete example which testifies to the fact that

¹⁰⁹In carrying out this estimate use was made of $a_{eff} = (R(^{11}\text{Li})/R_0(^{11}\text{Li}))a$ (within this context see Fig. 3.2.2).

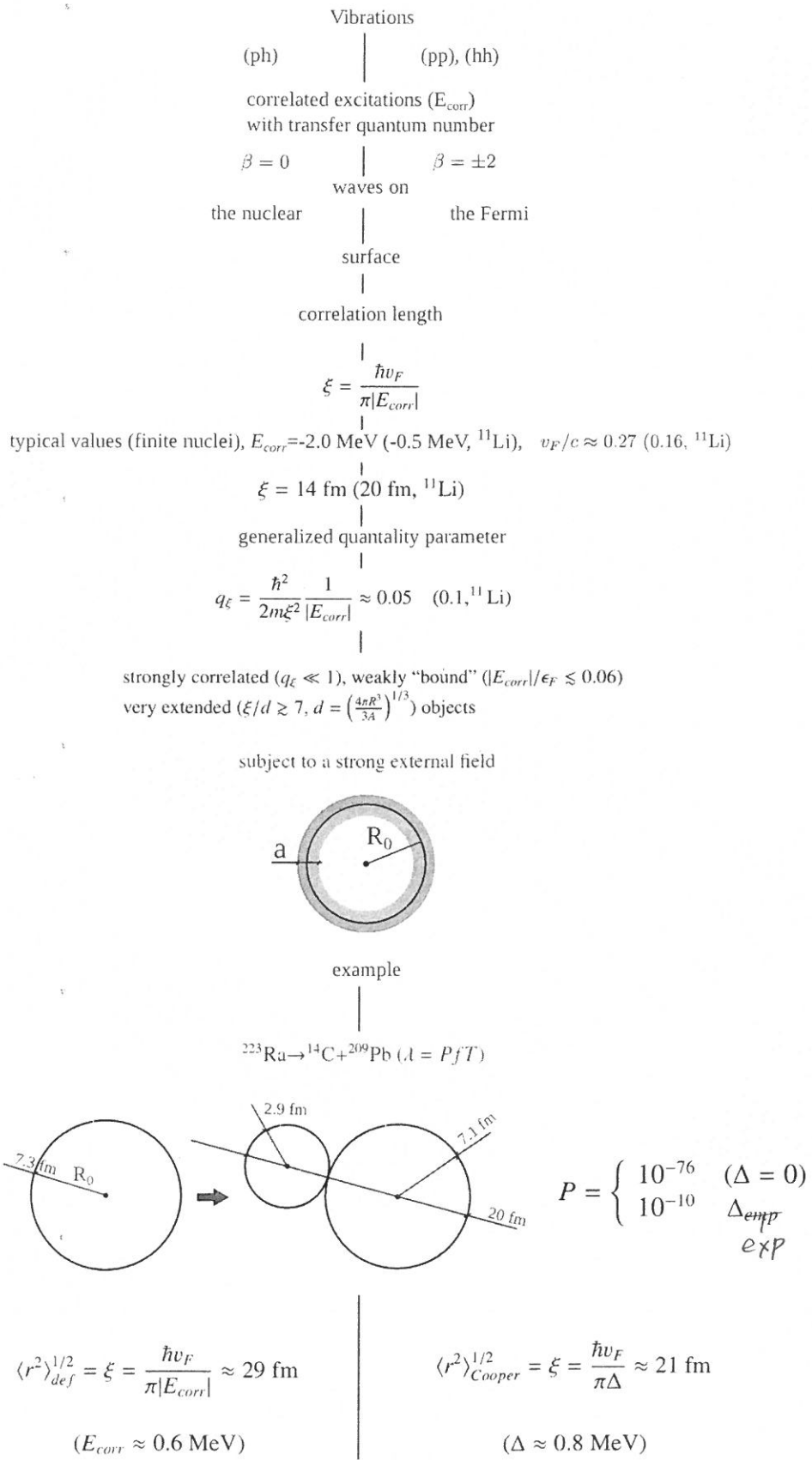


Figure 3.B.3

(*ph*) excitations (large amplitude surface distortion) and independent pair motion (superfluidity) are correlated over dimensions larger than typical nuclear dimensions, is provided by e.g. fission and exotic decay, in particular $^{223}\text{Ra} \rightarrow ^{14}\text{C} + ^{209}\text{Pb}$. In the related estimates use has been made of¹¹⁰ $\Delta = 12/\sqrt{A}$ MeV; $C = 18.1$ MeV, $D/\hbar^2 = 29.1$ MeV⁻¹ and¹¹¹ $\hbar\omega = \hbar(C/D)^{1/2} \approx 0.8$ MeV; $E = 1.4$ MeV, while¹¹² $E_{corr} = -(E - \hbar\omega)$. In keeping with the uncertainties affecting the above simple estimates (factor 2 or π in the denominator of ξ , $\langle r^2 \rangle_{Cooper}^{1/2}$, $\sqrt{\frac{5}{3}}\langle r^2 \rangle_{Cooper}^{1/2}$, etc.), it seems fair to conclude that $(15) \lesssim \xi \lesssim (25)$. Thus, one is likely faced with an intermediate situation in which $2 \lesssim \xi/R \lesssim 3$.

$15 \text{ fm} \lesssim \xi \lesssim 25 \text{ fm}$

¹¹⁰Bohr and Mottelson (1969).

¹¹¹Brink, D. and Broglia (2005) Sect. 7.1.

¹¹²Bohr, A. and Mottelson (1975) Fig. 6-38.